EJN fens EUROPEAN JOURNAL OF NEUROSCIENCE

European Journal of Neuroscience, Vol. 38, pp. 3181–3188, 2013 doi:10.1111/ejn.12338

NEUROSYSTEMS

Energy-efficient encoding by shifting spikes in neocortical neurons

Aleksey Malyshev,[1,2] Tatjana Tchumatchenko,[3] Stanislav Volgushev[4,5] and Maxim Volgushev[1,2]
[1]Department of Psychology, University of Connecticut, 406 Babbidge Road, Unit 1020, 06269-1020 Storrs, CT, USA
[2]Institute of Higher Nervous Activity and Neurophysiology, RAS, Moscow, Russia
[3]Max Planck Institute for Brain Research, Frankfurt am Main, Germany
[4]Faculty for Mathematics, Ruhr-University Bochum, Bochum, Germany
[5]Department of Statistics, University of Illinois, Urbana-Champaign, IL, USA

Keywords: population coding, rat neocortex, response speed, signal detection time, slices

Abstract

The speed of computations in neocortical networks critically depends on the ability of populations of spiking neurons to rapidly detect subtle changes in the input and translate them into firing rate changes. However, high sensitivity to perturbations may lead to explosion of noise and increased energy consumption. Can neuronal networks reconcile the requirements for high sensitivity, operation in a low-noise regime, and constrained energy consumption? Using intracellular recordings in slices from the rat visual cortex, we show that layer 2/3 pyramidal neurons are highly sensitive to minor input perturbations. They can change their population firing rate in response to small artificial excitatory postsynaptic currents (aEPSCs) immersed in fluctuating noise very quickly, within 2–2.5 ms. These quick responses were mediated by the generation of new, additional action potentials (APs), but also by shifting spikes into the response peak. In that latter case, the spike count increase during the peak and the decrease after the peak cancelled each other, thus producing quick responses without increases in total spike count and associated energy costs. The contribution of spikes from one or the other source depended on the aEPSCs timing relative to the waves of depolarization produced by ongoing activity. Neurons responded by shifting spikes to aEPSCs arriving at the beginning of a depolarization wave, but generated additional spikes in response to aEPSCs arriving towards the end of a wave. We conclude that neuronal networks can combine high sensitivity to perturbations and operation in a low-noise regime. Moreover, certain patterns of ongoing activity favor this combination and energy-efficient computations.

Introduction

Accumulating evidence suggests that cortical networks use sparse code for representing sensory stimuli and processing. Sparseness means that information is encoded by the activity of a small subpopulation of neurons, and often in a few, temporally precise spikes (Theunissen, 2003; Olshausen & Field, 2004; Wolfe *et al.*, 2010). Examples of sparse coding in the brain range from representation of visual objects and scenes, sounds and somatosensory information in respective sensory cortices (e.g. Olshausen & Field, 1996; Brecht & Sakmann, 2002; Lewicki, 2002) and odors in the olfactory bulb (Spors & Grinvald, 2002), to feedback projections from motor to sensory cortices (Petreanu *et al.*, 2012) and decision-making networks of the parietal cortex (Harvey *et al.*, 2012). Although cortical synapses can occasionally be strong (Miles & Wong, 1983; Volgushev *et al.*, 1995; Galarreta & Hestrin, 2001; Song, 2005; Lefort *et al.*, 2009; IkegayaY *et al.*, 2013), the vast majority of connections between cortical neurons are weak. To achieve sparse coding using these weak connections, neurons need to be sensitive to subtle changes in their inputs. Indeed, recent studies have shown that neocortical neurons are highly sensitive to even minor perturbations at their inputs (London *et al.*, 2010; Tchumatchenko *et al.*, 2011; Ilin *et al.*, 2013). Moreover, neurons can change their firing rate in response to small-amplitude current steps embedded in the fluctuating input very quickly, on the scale of 1–2 ms (Tchumatchenko *et al.*, 2011; Ilin *et al.*, 2013). However, in a system composed of highly sensitive elements, any perturbation, including noise, may be amplified, leading to a 'noise explosion' (London *et al.*, 2010). A high level of noise would necessitate the use of strong signals for communication between neuronal ensembles, and create unfavorable conditions for temporal coding, thus forcing the use of rate coding (London *et al.*, 2010). It would also lead to increased energy consumption, which is an important constraint on the processing abilities of the brain (Attwell & Laughlin, 2001; Lennie, 2003; Harris *et al.*, 2012). It remains unclear whether high sensitivity to perturbations is compatible with operation in a low-noise regime that favors sparse temporal coding. Here, we show, using intracellular recordings in slices from the rat visual cortex, that layer 2/3 pyramidal

Correspondence: M. Volgushev, [1]Department of Psychology, as above.
E-mail: maxim.volgushev@uconn.edu

Received 12 April 2013, revised 2 July 2013, accepted 14 July 2013

neurons can respond to small artificial excitatory postsynaptic currents (aEPSCs) by changing their population firing rate very quickly, within ~2 ms after the excitatory postsynaptic current (EPSC) onset. A quick increase in the firing rate was produced by the generation of new, additional action potentials (APs) but also by shifting spikes into the response peak. Neurons typically responded by shifting spikes to aEPSCs arriving at the beginning of a depolarization wave. Because these responses did not lead to an increase in total spike count, they would not lead to an explosion of firing, and increases in noise and related energy costs in the system. We conclude that neuronal networks can combine both high sensitivity to perturbations and operation in a low-noise regime, and that certain patterns of ongoing activity are especially favorable for this combination and for energy-efficient computations.

Materials and methods

All experimental procedures used in this study were in accordance with National Institutes of Health regulations. Experimental protocols were approved by the Institutional Animal Care and Use Committee of the University of Connecticut. *In vitro* intracellular recordings were made in slices of rat visual cortex. The details of slice preparation and recording were similar to those described previously (Volgushev *et al.*, 2000; Tchumatchenko *et al.*, 2011; Ilin *et al.*, 2013). Wistar rats (postnatal day 21–28; Charles River or Harlan, USA) were anesthetized with isoflurane (Baxter, USA) and decapitated, and the brain was rapidly removed. One hemisphere was mounted onto an agar block, and 350-μm-thick coronal slices containing the visual cortex were cut with a vibrotome (Leica, Germany) in ice-cooled oxygenated solution. After being cut, the slices were placed into an incubator, where they were allowed to recover for at least 1 h at room temperature before being transferred to the recording chamber. The solution used during the preparation of the slices had the same ionic composition as the perfusion/extracellular solution. It contained 125 mM NaCl, 2.5 mM KCl, 2 mM $CaCl_2$, 1 mM $MgCl_2$, 1.25 mM NaH_2PO_4, 25 mM $NaHCO_3$, and 25 mM D-glucose, and was bubbled with 95% O_2 and 5% CO_2. In some experiments, synaptic transmission was blocked by adding 25 μM 2*R*-amino-5-phosphonopentanoate, 5 μM 6,7-dinitroquinoxaline-2,3-dione and 80 μM picrotoxin to the extracellular solution. Chemicals were obtained from Sigma-Aldrich or Tocris.

Recordings were made with the slices submerged at 28–32 °C. The temperature in the recording chamber was monitored with a thermocouple positioned close to the slice, 2–3 mm from the recording site. Whole-cell recordings with patch electrodes were made from layer 2/3 pyramidal neurons, selected under visual control with Nomarski optics and infrared videomicroscopy. The patch electrodes were filled with a potassium gluconate-based solution (130 mM potassium gluconate, 20 mM KCl, 4 mM Mg-ATP, 0.3 mM Na_2-GTP, 10 mM sodium phosphocreatine, 10 mM Hepes) and had a resistance of 4–6 MΩ. Recordings were performed with the bridge mode of an Axoclamp-2A (Axon Instruments, USA) or a Dagan BVC-700A (Dagan Corporation, USA) amplifier. After amplification and low-pass filtering at 10 kHz, data were digitized at 20 kHz and fed into a computer (Pentium4; Digidata 1440A interface and PCLAMP software; Molecular Devices).

Fluctuating current for injection into a neuron, $\sigma\eta(t)$, was synthesized to mimic the effect produced in the soma by numerous balanced excitatory and inhibitory synaptic inputs (Destexhe & Pare, 2003). $\eta(t)$ was an Ornstein–Uhlenbeck process with zero mean, unit variance and correlation time $\tau_1 = 50$ ms, and σ was the standard deviation of the resulting background current noise, scaled to achieve membrane potential fluctuations of ~15–20 mV in amplitude. Membrane potential fluctuations produced by the injected current were similar to those recorded in neocortical neurons *in vivo* (Azouz & Gray, 2000; Destexhe & Pare, 2003; Volgushev *et al.*, 2003, 2006). Each realization of the noise current was injected either as 'noise only', or with aEPSCs added at a rate of 1/s (Fig. 1B and C). aEPSCs were synthesized with a rise time of 1 ms, a decay time of 10 ms, and a peak amplitude of 20 pA. During current

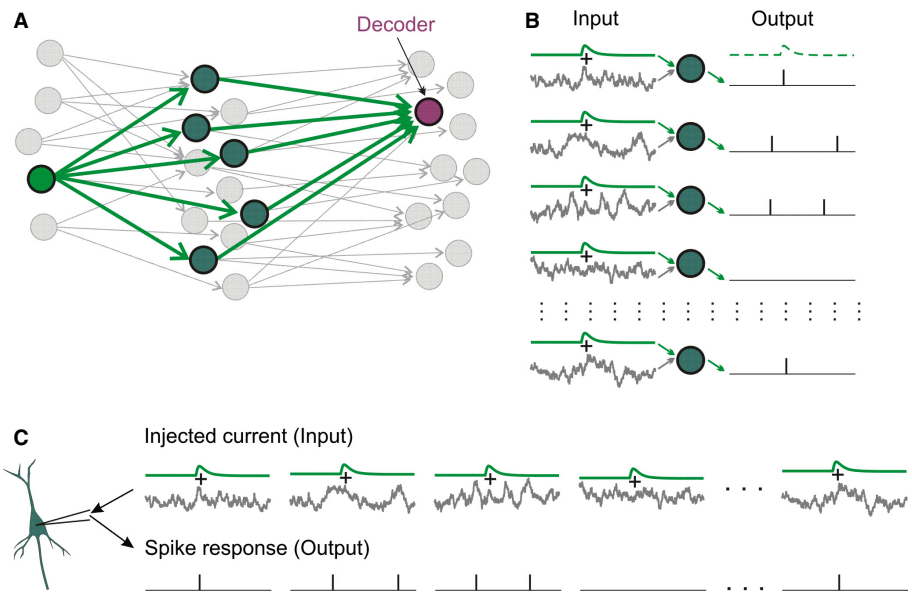

FIG. 1. Experimental paradigm – how to study population encoding in slices. (A) A scheme of the three-layer network of neurons. Green arrows show divergent connections from one-first-layer neuron ('source neuron') with neurons of the second layer, which converge on a third-layer neuron ('decoder'). Other neurons and connections are shown in gray. (B) The input to each second-layer neuron consists of individual fluctuating noise and a common EPSC produced by an AP in the source neuron. Population firing of these neurons provides synaptic input to the decoder neuron in the third layer. (C) In the experiment, aEPSCs immersed in different episodes of fluctuating noise are injected in a cell sequentially. This mimics population encoding from (B). [Color version of figure available online].

injection, a DC current was added if necessary to maintain the desired firing rate of ~4–5 Hz in most experiments, or ~1 Hz in some experiments, as indicated. All currents were injected into the soma through the whole-cell recording pipette. Current injections lasted for 46 s, and were separated by a recovery period of 60–100 s.

Data were processed offline in MATLAB (The Mathworks, Natick, MA, USA). Spikes were detected in membrane potential traces as positive zero crossings. Spike timings were used for construction of peristimulus time histograms (PSTHs), and for estimating EPSC detection probability.

The probability of EPSC detection was quantified with a theoretical decoder (Tchumatchenko *et al.*, 2011; Ilin *et al.*, 2013) that reports a change in the input when the population firing rate exceeds the 95% quantile of the pre-signal distribution. The probability of detection was estimated as function of time interval T (from 0.4 ms to 10 ms after the EPSC onset), for populations of 300, 1000 and 3000 neurons, with bootstrap analysis, and calculated from theoretical distributions. For bootstrap analysis, we composed 100 trial sets of 300 (or 1000 or 3000) randomly selected sweeps. For each time interval T, we first used all 100 trial sets to calculate the distribution of spike counts during the pre-signal interval T and defined the 95% quantile of this distribution. Next, for each trial set, we determined whether the spike count in the interval T after the EPSC onset fell outside the 95% quantile of the pre-signal distribution. The number of trial sets that fulfill this condition provides an estimate of the probability of a population of N neurons detecting the EPSC within time T after its onset. The whole procedure was then repeated 30 times for 300 (or 1000 or 3000) neurons to obtain the results shown as open circles in Fig. 2D.

Theoretical curves of detection probability were calculated as follows. The distribution of the number of spikes in a window of length T after the signal onset, D_{post}, and the distribution of the number of spikes in a window of the same length before signal onset, D_{pre}, were modeled as two independent binomial distributions with N equal to the number of neurons ($N = 300$, $N = 1000$, or $N = 3000$), and success probabilities P_{post} (after EPSC onset) and P_{pre} (before EPSC onset), respectively. The success probabilities P_{post} and P_{pre} were estimated by using data from all recordings as average probabilities of spikes, i.e.

$$(\text{total number of spikes in window } T)/(\text{total number of repetitions})$$

The theoretical detection probabilities were then computed as the probability that a binomial distribution $B(N,P_{post})$ exceeds the 95% quantile of a binomial distribution $B(N,P_{pre})$, i.e.

$$1 - F_{B(N,P\text{post})}[F^{-1}_{B(N,P\text{pre})}(0.95)]$$

with $F_{B(N,P\text{post})}$ and $F^{-1}_{B(N,P_{pre})}$ denoting the distribution and quantile function of a binomial random variable with parameters N and P, respectively. Distributions and quantiles were computed with the MATLAB programs *binoinv* and *binocdf*.

The significance of an increase or decrease in spike count in response to the injection of fluctuating currents with immersed aEPSCs as compared with responses to currents without aEPSCs was calculated on the basis of on a one-sided version Welch's t-test. Spike count was considered to be significantly ($P < 0.05$) increased (decreased) if the lower (upper) bound of the one-sided confidence interval for the difference of the mean spiking rate was above (below) zero.

Results

We used an established approach to study firing rate responses of neuronal populations (Silberberg *et al.*, 2004; Tchumatchenko *et al.*, 2011; Ilin *et al.*, 2013). Consider a population of independent

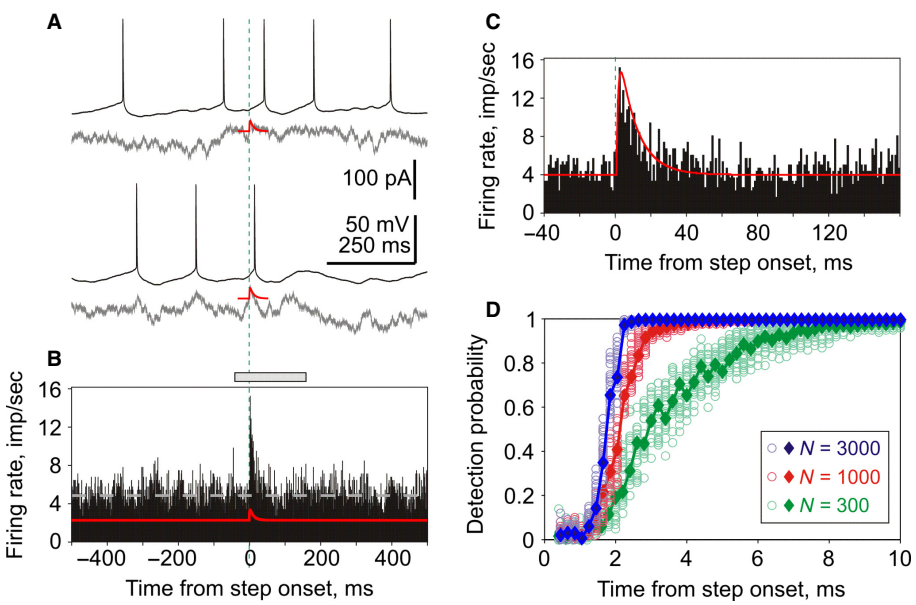

FIG. 2. Rapid detection of small aEPSCs in population firing. (A) Responses of a neocortical neuron to injection of two episodes of fluctuating noise current (gray traces) with immersed small aEPSCs (red). (B) Firing rate changes of a neuronal population in response to injection of fluctuating current with immersed aEPSCs (red trace). Data from 11 neurons; total of 2959 repetitions. Bin 1 ms. The dashed gray line shows averaged firing rate (4.84 impulses/s). (C) Zoom-in of response peak, a portion of the histogram indicated by the gray bar at the top of (B). Green vertical dashed lines in (A–C) show aEPSC onset. (D) Probability of aEPSC detection by populations of 300, 1000 and 3000 neurons vs. time – results of bootstrapping (circles) and theoretical curves (diamonds, solid lines). [Color version of figure available online].

neurons receiving input from one common fiber (Fig. 1A). Each neuron of the population has a unique pattern of background activity ('noise') that is different from that of other neurons, but also receives an input from a common fiber, which is the same for all neurons in the population (Fig. 1B). Background activity in each neuron is mimicked by injecting fluctuating noise current, which is different for different cells, and common input is mimicked by introducing a common signal, an aEPSC injected into all neurons. Recording from all neurons of the population simultaneously (Fig. 1B) is mathematically equivalent to successive recording of responses of several cells to the signal immersed in different realizations of the fluctuating noise (Fig. 1C). Averaging the successively recorded responses provides an estimate of the population response, whereby the number of repetitions is equivalent to the number of neurons in the population (Silberberg *et al.*, 2004).

Figure 2A shows membrane potential responses to the injection of two different realizations of fluctuating noise with immersed aEPSCs. The PSTH constructed with spikes from 2959 such responses shows a clear peak at the aEPSC onset (Fig. 2B and C). The firing rate changes sharply within ~2 ms after the aEPSC onset. A theoretical decoder that reports a change in the input if the population firing rate exceeds the 95% quantile of the pre-signal distribution (Ilin *et al.*, 2013) can report the change in firing rate of a population of 1000 or 3000 neurons very quickly, within 2–2.5 ms (Fig. 2D). With a decrease in the size of the population to 300, the time required for detection increases to approximately 5–6 ms (Fig. 2D, green). The high sensitivity of neocortical neurons to aEPSCs described above is consistent with recent *in vivo* (London *et al.*, 2010) and *in vitro* (Tchumatchenko *et al.*, 2011) results. Also, the quantification of the detection speed of aEPSCs and its dependence on the size of neuronal population are in agreement with recent reports on quick detection of small DC current steps by populations of neocortical neurons *in vitro* (Tchumatchenko *et al.*, 2011; Ilin *et al.*, 2013).

However, high sensitivity of neurons to input perturbations and high speed of firing rate responses to subtle changes in the input may have undesirable effects on the operation of neuronal networks. The generation of new spikes in response to any additional EPSC may lead to amplification of random perturbations, and thus to 'noise explosion' in the system (London *et al.*, 2010) and a corresponding increase in energy consumption. It remains unclear how these undesirable effects are counteracted in neuronal networks. One possibility here is to change the timing of spikes, so that APs that are about to be generated at some time during the next few dozens of milliseconds will be actually generated earlier, upon arrival of an additional EPSC. In this scenario, the EPSC would still produce a peak in the population firing rate, but would not lead to additional spikes and related undesirable network effects. This 'redistribution' hypothesis predicts that: (i) after the EPSC-produced peak, the firing rate will decrease below the average; and (ii) the number of spikes in the histogram peak will be higher than the total increase in the spike count.

To test these predictions, we injected neurons with pairs of fluctuating currents – one sweep consisting of fluctuating noise with aEPSCs immersed in it, as in the experiments described above, and the other sweep in a pair containing the same fluctuating noise only, without aEPSCs. Figure 3A shows the firing rate changes of a large population of neurons (N = 12 105; mean firing rate, 4.2 Hz) in response to injection of fluctuating noise with and without an immersed aEPSC. Because injections of fluctuating current induce reliable and reproducible spike responses in neocortical neurons (Mainen & Sejnowski, 1995), the difference between the two

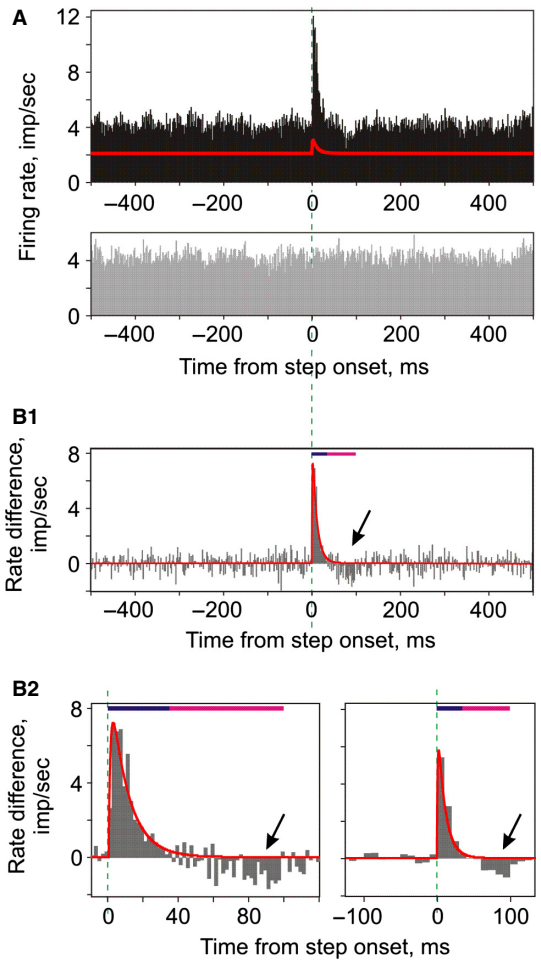

FIG. 3. The transient firing rate response to small aEPSCs is produced both by generation of additional APs and by shifting the 'existing' spikes. (A) Firing rate changes of a large neuronal population (data from 17 neurons,12 105 repetitions; bin 2 ms) in response to injection of fluctuating current with immersed aEPSCs (top), and responses to the same fluctuating current but without aEPSCs (gray histogram, bottom). (B1, B2) Difference between population firing induced by injection of fluctuating current with and without aEPSCs, calculated with data from (A). The red line shows the aEPSC, scaled to match the amplitude of the histogram peak. (B2) Zoom-ins of the peak region (left) and histogram with the 10-ms bin (right). In all three histograms in B1, B2, dark blue bars show the duration of the aEPSC and the histogram peak (0–35 ms), and the magenta bars show the period of decreased firing (arrows, 35–100 ms). [Color version of figure available online].

histograms (Fig. 3B) provides an estimate of the firing rate change caused by the addition of aEPSCs relative to control. The difference histogram demonstrates, first, that the shape of the histogram peak (0–35 ms after the aEPSC onset) reproduces precisely the shape of the injected aEPSC, and second, that there is a decrease in the firing rate after the peak during 35–100 ms after the aEPSC onset (oblique arrows in Fig. 3B1 and B2). The decrease in population firing rate stands out clearly in the zoom-in of the response and with a larger bin size (Fig. 3B2). It indicates that some of the spikes generated in the noise-only condition did not appear during 35–100 ms of responses to aEPSCs immersed in noise. Moreover, the increase in total spike count in response to injection of noise with aEPSCs as compared with noise only (N_{new} = 781 spikes) was less than the number of spikes in the peak (0–35 ms, N_{peak} = 1146 spikes). Thus, the response peak was composed of APs originating from two sources. Of 1146 spikes in the response peak, approximately

two-thirds were 'new' or 'additional' spikes, which would not be generated in response to injection of noise current without an aEPSC (N_{new} = 781, or 68% of N_{peak} = 1146). The remaining one-third of the response peak was composed of 'shifted' spikes, i.e. those that would be generated in response to noise-only injection, but the addition of an aEPSC changed their timing, shifting them into the response peak ($N_{shifted} = N_{peak} - N_{new}$ = 365, or 32% of N_{peak} = 1146). The effect of shifting spikes into the response peak by the addition of an aEPSC was also clearly present in experiments with a lower rate of background firing (1.1 Hz, $N_{shifted}$ = 229, or 22% of N_{peak} = 1065). These results are consistent with the above predictions of the redistribution hypothesis.

What determines whether the response to an aEPSC is composed of added or shifted spikes? To address this question, we exploited the fact that the peak of the population response reproduces precisely the shape of an aEPSC (Fig. 3). This allowed us to specify, for the following analysis, two intervals – one that included the peak (0–35 ms after aEPSC onset), and another that included the trough of the firing rate response (35–100 ms). The generation of additional APs in response to aEPSCs would produce a histogram peak that would not be followed by a decrease in the firing rate below the mean. In contrast, shifting spikes into the peak would lead to a firing rate decrease after the peak. In the next series of experiments, we repeatedly injected, in five neurons, 45 pairs of episodes of fluctuating noise with or without immersed aEPSCs (Fig. 4A). Each pair of episodes was injected 110 times. For each pair, we computed difference histograms (Fig. 4B). Note that the histograms in each column were computed by using responses to multiple injections of the same realization of the fluctuating current. For this reason, noise-only histograms are not flat, and the difference histograms in Fig. 4B do not reproduce the aEPSC shape. However, because the firing rate response of a population of neurons receiving independent fluctuating input reliably reproduces the aEPSC shape (Fig. 3), we used the windows defined above to calculate changes in spike count during the response peak (0–35 ms; Fig. 4B) and during the trough (35–100 ms; Fig. 4B). Figure 4B illustrates four types of difference histogram. Histograms of the first type showed an increase in the firing rate during 0–35 ms after aEPSC onset ($P < 0.05$), followed by a comparable decrease in the firing rate below the mean level during the 35–100-ms interval (Fig. 4B, left column). The histogram peak was thus produced by shifting the spikes that would occur later in response to noise-only current injection. In histograms of the second type, the increase in the firing rate during 0–35 ms was not followed by a significant decrease during

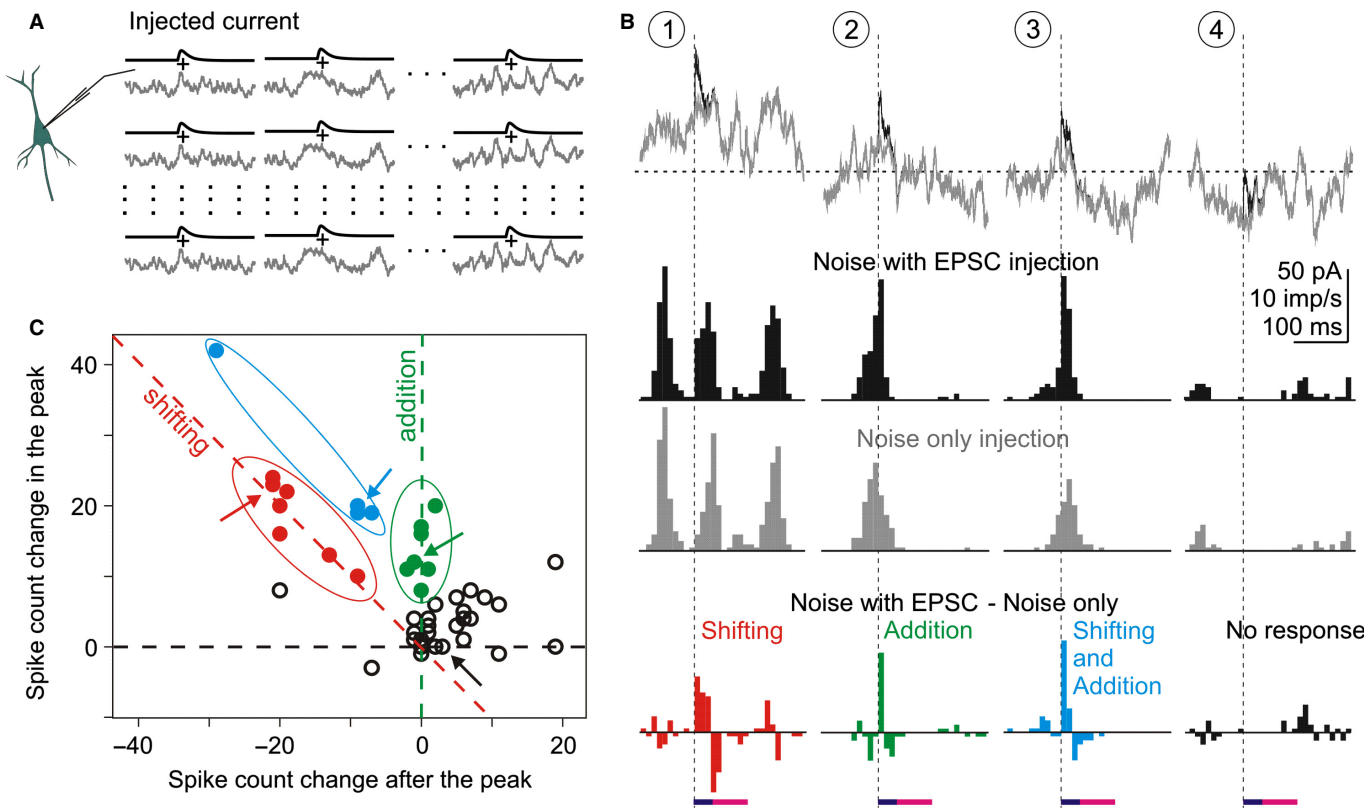

FIG. 4. Differential contributions of added and shifted spikes to the histogram peak. (A) Experimental paradigm. A set of 45 different episodes of fluctuating noise with or without immersed aEPSCs were injected into neurons repeatedly (110 repetitions). (B) Examples of four (out of 45) episodes of the injected currents and firing rate responses. Gray traces of noise without aEPSCs are superimposed on black traces with immersed aEPSCs; vertical dashed lines show aEPSC onset. The horizontal dashed line shows the DC current (0.255 nA) used to achieve a target firing rate of 4–6 impulses/s. Histograms show firing rate responses to the injected currents with (black) or without (gray) immersed aEPSCs, and their difference (colored histograms). The horizontal bars in the bottom show measuring windows corresponding to the duration of the aEPSC/histogram peak (dark blue, 0–35 ms), and the period of decreased firing (magenta, 35–100 ms), as in Fig. 3B. For each of the 45 difference histograms, the number of spikes was measured in these windows. (C) Spike count in the peak (0–35 ms) vs. spike count after the peak (35–100 ms) of 45 difference histograms. Red symbols (n = 7) show cases when spikes were 'shifted' to produce the histogram peak – the spike number increase in the histogram peak was balanced by the decrease after the peak. Green symbols (n = 7) show cases in which the histogram peak was produced by additional, 'new' spikes – spike count was increased in the peak but did not change after the peak. Blue symbols (n = 4) show cases with both added and shifted spikes. Open symbols show the remaining (n = 27) cases. Arrows indicate data for four episodes from (B). [Color version of figure available online].

the 35–100-ms interval, indicating that the aEPSC led to the generation of additional spikes that were not present in the response to noise-only injection (Fig. 4B, second column). In histograms of the third type, the peak was followed by a firing rate decrease, but the decrease was of a smaller magnitude than the peak. We interpreted this as an indication that both additional and shifted spikes contributed to the peak (Fig. 4B, third column). Finally, histograms of the fourth type showed little aEPSC-related firing rate change. In fact, on most such occasions, neither injection of noise-only current nor injection of noise with aEPSCs evoked spikes during the specified intervals (Fig. 4B, right column).

The scatter plot in Fig. 4C shows the results of this analysis for all 45 episodes. Each point represents the data for one pair of noise episodes, with the spike count change in the peak (0–35 ms after aEPSC onset) plotted against spike count change during the 35–100-ms interval. Note that calculations were performed with the difference histograms, so spike count values can be negative. When the histogram peak was produced by shifting spikes, that is, the increase in spike count during the peak was compensated by the decrease in spike count in the 35–100-ms interval (type 1 histogram), data points were located at or around the negative-slope diagonal (Fig. 4C). When the peak was produced by added spikes (type 2 histogram), respective data points were located around the ordinate (Fig. 4C). Data points located between the negative-slope diagonal and the ordinate represent cases in which the histogram peak was composed of both added and shifted spikes (type 3 histogram).

We thought that the reason why an aEPSC led to additional spikes in some cases but shifted spikes into the peak in other cases may lay in the difference between patterns of the ongoing membrane potential fluctuations during which aEPSCs arrived. To test this conjecture, we selected seven cases in which the histogram peak was produced by shifted spikes, seven cases in which the peak was formed by additional spikes, and four cases in which both added and shifted spikes contributed to the peak (Fig. 4C). For each of the three groups, we computed the PSTHs and averaged traces of the membrane potential (Fig. 5). The pattern of background activity was clearly different for the three groups. When aEPSCs arrived at the beginning of a depolarizing wave and the associated increase in population firing, they shifted the spikes into the response peak (Fig. 5, left column). When they arrived towards the end of a depolarizing wave, they evoked additional spikes (Fig. 5, middle column). When they arrived in the middle of the activity wave, they shifted spikes and evoked additional ones (Fig. 5, right column). Thus, the pattern of ongoing activity determines whether additional spikes will be generated in response to an EPSC, or whether a neuron will respond by shifting the spikes, without a net increase in the firing rate.

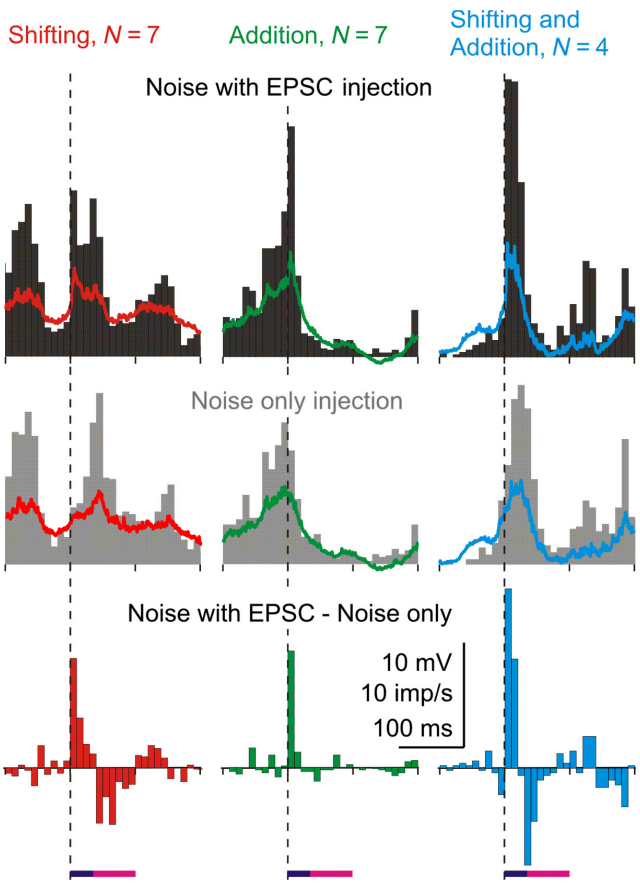

FIG. 5. Relative contributions of added and shifted spikes to the response peak depend on the pattern of background activity. Firing rate changes in episodes in which the response peak was composed of shifted spikes (n = 7, left column), added spikes (n = 7, middle column) and a combination of shifted and added spikes (n = 4, right column). Responses to injection of fluctuating noise with aEPSCs, noise only and their difference are shown. Averaged membrane potential traces are superimposed on the respective histograms. Dashed vertical lines show the onset of aEPSCs.

Discussion

The results of the present study show that populations of cortical neurons are highly sensitive to even minor perturbations of their input, and can change their firing rate very quickly, within 2–2.5 ms, in response to small aEPSCs. Quick firing rate responses to aEPSCs were mediated by: (i) the generation of new, additional APs; and (ii) shifting spikes into the peak, so that the increased spike count during the response peak was compensated by the decrease in the number of spikes that occurred after the peak. The contribution of spikes from one or the other source to the response peak depended on the EPSC timing relative to the pattern of ongoing activity.

The high sensitivity of neocortical neurons to small aEPSCs is consistent with recent results reported for neurons of other types and/or from other cortical regions (London *et al.*, 2010; Tchumatchenko *et al.*, 2011). In pyramidal neurons from layer 5 of the rat barrel cortex *in vivo*, injection of subtle aEPSCs (~25 pA in amplitude) led to a detectable change in the firing of neurons. Moreover, APs induced in a single neuron by depolarizing pulses led to a measurable change in the population firing of neighboring neurons (London *et al.*, 2010). In layer 3 pyramidal neurons from the rat visual cortex *in vitro*, injection of small current steps immersed in fluctuating noise led to clear changes in population firing that could be detected quickly, on a millisecond time scale (Tchumatchenko *et al.*, 2011; Ilin *et al.*, 2013). Prior data have also shown that neocortical neurons connected via strong synapses (~180 pA in amplitude) can communicate rapidly (Galarreta & Hestrin, 2001), and that a few strong connections may define the preferred pathways for transmission of sensory information in neocortical networks (Lefort *et al.*, 2009; Teramae *et al.*, 2012; Ikegaya *et al.*, 2013). Our results extend these findings, showing that populations of neocortical neurons can respond to small EPSC-shaped signals immersed in fluctuating noise by changing their firing rate quickly, within ~2 ms after aEPSC onset. This demonstrates that weak synaptic connections can effectively influence neuronal firing, and thus the propagation of signals in neocortical networks. Moreover, neocortical neuronal ensembles are able to communicate rapidly, on a millisecond time scale, using weak signals. High sensitivity to subtle changes in the input and the ability to communicate rapidly by using

weak signals are vital features for sparse encoding in cortical networks (Olshausen & Field, 1996, 2004; Theunissen, 2003; Wolfe *et al.*, 2010).

The downside of the high sensitivity is that any perturbation, including noise, can lead to firing rate changes. In multilayer networks consisting of highly sensitive elements, this may lead to amplification of signal-irrelevant events, resulting in a 'noise explosion' (London *et al.*, 2010), runaway firing, and eventually to overexcitation in the system. These effects would have devastating consequences for the operation of neural networks. Increased noise would lead to a degradation of the signal-to-noise ratio, necessitating stronger signals for processing. The increased firing rate and the demand for stronger signals would lead to a dramatic increase in energy consumption. The generation of each AP is associated with a chain of energy-demanding processes, such as the restoration of ionic gradients disturbed by currents involved in the initiation and propagation of the AP, transmitter release, and postsynaptic currents, that, in total, account for ~50 to ~70% of energy consumption in the cortex (Attwell & Laughlin, 2001; Lennie, 2003; Harris *et al.*, 2012; Howarth *et al.*, 2012). These undesirable consequences may occur when neurons respond to changing inputs by generating additional APs. Explosion of activity can be prevented by inhibition – ample evidence indicates that cortical neuronal networks operate in a balanced regime (van Vreeswijk & Sompolinsky, 1996; Okun & Lampl, 2008; Ozeki *et al.*, 2009). Our results indicate an additional mechanism that helps to prevent explosion of noise and the metabolic costs of computations in neuronal networks. When firing rate responses to EPSCs are mediated by shifting spikes into the response peak, these problems do not occur at all. Because the net number of spikes generated by a population of neurons does not change, neither the noise in the system nor energy consumption will increase. Rather, the response will be manifested as a redistribution of the neuronal activity, so that the refined firing pattern will incorporate information about the EPSC and its timing.

In our experiments, approximately one-third of the response peak in the PSTH was attributable to shifted spikes. How can spike timing be shifted? We hypothesized that, when a neuron is about to generate a spike in response to injection of fluctuating noise, addition of an EPSP may advance the timing of the spike initiation, thus 'shifting' it into the response peak. Once the spike is generated, it raises the threshold for the generation of further spikes, thus leading to a trough in the histogram after the response peak. This interpretation is consistent with *in vivo* data showing that the AP threshold is influenced by the history of membrane potential changes during a few dozens of milliseconds, and cell firing during ~1 s preceding the spike (Azouz & Gray, 1999; Henze & Buzsaki, 2001).

The contribution of shifted vs. added spikes to the response peak depended on the pattern of ongoing activity. Activities of neuronal ensembles across various brain regions and states show a distinct temporal structure, examples ranging from the hippocampal theta rhythm during active exploration (Buzsaki, 2006) or responses to sensory stimuli (e.g. Volgushev *et al.*, 2003) to slow sleep waves (Steriade & Timofeev, 2003; Chauvette *et al.*, 2011). Activation of a single inhibitory neuron can completely shunt AP generation or shift its timing in pyramidal neurons in the hippocampus (Cobb *et al.*, 1995; Miles *et al.*, 1996). Our present results show that excitatory inputs, activated at certain phases of the ongoing rhythm, can also produce a clear, detectable change in the firing rate mediated by a change in the timing of APs, without the generation of additional spikes. In this regime, despite the high sensitivity of neurons to input perturbations (Galarreta & Hestrin, 2001; London *et al.*, 2010; Tchumatchenko *et al.*, 2011), the noise level would remain low, as would the metabolic costs of neuronal computations (Attwell & Laughlin, 2001; Lennie, 2003; Harris *et al.*, 2012). Redistribution of discharges of neuronal populations rather than the generation of additional spikes may be one mechanism for the refinement of the firing pattern of neuronal ensembles – a desirable feature for a multitude of neural functions that rely on the precise timing of spikes, such as spike timing-dependent synaptic plasticity (Caporale & Dan, 2008), or effective temporal coding in sensory processing (Gray & Singer, 1989; Singer, 1999).

Acknowledgements

We are grateful to Marina Chistyakova, James Chrobak and Harvey Swadlow for comments on the manuscript. T. Tchumatchenko was supported by a fellowship from the Volkswagen Foundation; S. Volgushev was supported by a fellowship from the German Research Foundation. This work was supported by a grant from the RFBR to A. Malyshev and grant R01MH087631 from the NIH and start-up funds from the University of Connecticut to M. Volgushev.

Abbreviations

aEPSC, artificial excitatory postsynaptic current; AP, action potential; EPSC, excitatory postsynaptic current; PSTH, peristimulus time histogram.

References

Attwell, D. & Laughlin, S.B. (2001) An energy budget for signaling in the grey matter of the brain. *J. Cerebr. Blood F. Met.*, **21**, 1133–1145.

Azouz, R. & Gray, C.M. (1999) Cellular mechanisms contributing to response variability of cortical neurons *in vivo*. *J. Neurosci.*, **19**, 2209–2223.

Azouz, R. & Gray, C.M. (2000) Dynamic spike threshold reveals a mechanism for synaptic coincidence detection in cortical neurons *in vivo*. *Proc. Natl. Acad. Sci. USA*, **97**, 8110–8115.

Brecht, M. & Sakmann, B. (2002) Dynamic representation of whisker deflection by synaptic potentials in spiny stellate and pyramidal cells in the barrels and septa of layer 4 rat somatosensory cortex. *J. Physiol.*, **543**, 49–70.

Buzsaki, G. (2006) *Rhythms of the Brain*. Oxford University Press, Oxford.

Caporale, N. & Dan, Y. (2008) Spike timing-dependent plasticity: a Hebbian learning rule. *Annu. Rev. Neurosci.*, **31**, 25–46.

Chauvette, S., Crochet, S., Volgushev, M. & Timofeev, I. (2011) Properties of slow oscillations during slow-wave sleep and anesthesia in cats. *J. Neurosci.*, **31**, 14998–15008.

Cobb, S.R., Buhl, E.H., Halasy, K., Paulsen, O. & Somogyi, P. (1995) Synchronization of neuronal activity in hippocampus by individual GABAergic interneurons. *Nature*, **378**, 75–78.

Destexhe, A. & Pare, D. (2003) The high-conductance state of neocortical neurons *in vivo*. *Nat. Rev. Neurosci.*, **4**, 739–751.

Galarreta, M. & Hestrin, S. (2001) Spike transmission and synchrony detection in networks of GABAergic interneurons. *Science*, **292**, 2295–2299.

Gray, C.M. & Singer, W. (1989) Stimulus-specific neuronal oscillations in orientation columns of cat visual cortex. *Proc. Natl. Acad. Sci. USA*, **86**, 1698–1702.

Harris, J.J., Jolivet, R. & Attwell, D. (2012) Synaptic energy use and supply. *Neuron*, **75**, 762–777.

Harvey, C.D., Coen, P. & Tank, D.W. (2012) Choice-specific sequences in parietal cortex during a virtual-navigation decision task. *Nature*, **484**, 62–68.

Henze, D.A. & Buzsaki, G. (2001) Action potential threshold of hippocampal pyramidal cells *in vivo* is increased by recent spiking activity. *Neuroscience*, **105**, 121–130.

Howarth, C., Gleeson, P. & Attwell, D. (2012) Updated energy budgets for neural computation in the neocortex and cerebellum. *J. Cerebr. Blood F. Met.*, **32**, 1222–1232.

Ikegaya, Y., Sasaki, T., Ishikawa, D., Honma, N., Tao, K., Takahashi, N., Minamisawa, G., Ujita, S. & Matsuki, N. (2013) Interpyramidal spike transmission stabilized the sparseness of recurrent network activity. *Cereb. Cortex*, **23**, 293–314.

Ilin, V., Malyshev, A., Wolf, F. & Volgushev, M. (2013) Fast computations in cortical ensembles require rapid initiation of action potentials. *J. Neurosci.*, **33**, 2281–2292.

Lefort, S., Tomm, C., Sarria, J.C.F. & Peterson, C.C.H. (2009) The excitatory neuronal network of the C2 barrel column in mouse primary somatosensory cortex. *Neuron*, **61**, 301–316.
Lennie, P. (2003) The cost of cortical computation. *Neuron*, **13**, 493–497.
Lewicki, M.S. (2002) Efficient coding of natural sounds. *Nat. Neurosci.*, **5**, 356–363.
London, M., Roth, A., Beeren, L., Haeusser, M. & Latham, P.E. (2010) Sensitivity to perturbations *in vivo* implies high noise and suggests rate coding in cortex. *Nature*, **466**, 123–127.
Mainen, Z.F. & Sejnowski, T.J. (1995) Reliability of spike timing in neocortical neurons. *Science*, **268**, 1503–1506.
Miles, R. & Wong, R.K. (1983) Single neurones can initiate synchronized population discharge in the hippocampus. *Nature*, **306**, 371–373.
Miles, R., Toth, K., Gulias, A.I., Hajos, N. & Freund, T.F. (1996) Differences between somatic and dendritic inhibition in the hippocampus. *Neuron*, **16**, 815–823.
Okun, M. & Lampl, I. (2008) Instantaneous correlation of excitation and inhibition during ongoing and sensory-evoked activity. *Nat. Neurosci.*, **11**, 535–537.
Olshausen, B.A. & Field, D.J. (1996) Emergence of simple-cell receptive field properties by learning a sparse code for natural images. *Nature*, **381**, 607–609.
Olshausen, B.A. & Field, D.J. (2004) Sparse coding of sensory inputs. *Curr. Opin. Neurobiol.*, **14**, 481–487.
Ozeki, H., Finn, I.M., Schaffer, E.S., Miller, K.D. & Ferster, D. (2009) Inhibitory stabilization of the cortical network underlies visual surround suppression. *Neuron*, **62**, 578–592.
Petreanu, L., Gutnisky, D.A., Huber, D., Xu, N.-L., O'Connor, D.H., Tian, L., Looger, L. & Svoboda, K. (2012) Activity in motor-sensory projections reveals distributed coding in somatosensation. *Nature*, **489**, 299–303.
Silberberg, G., Bethge, M., Markram, H., Pawelzik, K. & Tsodyks, M. (2004) Dynamics of population rate codes in ensembles of neocortical neurons. *J. Neurophysiol.*, **91**, 704–709.
Singer, W. (1999) Neuronal synchrony: a versatile code for the definition of relations? *Neuron*, **24**, 49–65.
Song, S., Sjostrom, P.J., Reigl, M., Nelson, S. & Chklovskii, D.B. (2005) Highly nonrandom features of synaptic connectivity in local cortical circuits. *PLoS Biol.*, **3**, e68.
Spors, H. & Grinvald, A. (2002) Spatio-temporal dynamics of odor representations in the mammalian olfactory bulb. *Neuron*, **34**, 301–315.
Steriade, M. & Timofeev, I. (2003) Neuronal plasticity in thalamocortical networks during sleep and waking oscillations. *Neuron*, **37**, 563–576.
Tchumatchenko, T., Malyshev, A., Wolf, F. & Volgushev, M. (2011) Ultrafast population encoding by cortical neurons. *J. Neurosci.*, **31**, 12171–12179.
Teramae, J.N., Tsubew, Y. & Fukai, T. (2012) Optimal spike-based communication in excitable networks with strong-sparse and weak-dense links. *Sci. Rep.*, **2**, 485.
Theunissen, F.E. (2003) From synchrony to sparseness. *Trends Neurosci.*, **26**, 61–64.
Volgushev, M., Voronin, L.L., Chistiakova, M., Artola, A. & Singer, W. (1995) All-or-none excitatory postsynaptic potentials in the rat visual cortex. *Eur. J. Neurosci.*, **7**, 1751–1760.
Volgushev, M., Vidyasagar, T., Chistiakova, M., Yousef, T. & Eysel, U.T. (2000) Membrane potential and spike generation in rat visual cortical slices during reversible cooling. *J. Physiol.*, **522**, 59–76.
Volgushev, M., Pernberg, J. & Eysel, U.T. (2003) Gamma-frequency fluctuations of the membrane potential and response selectivity in visual cortical neurons. *Eur. J. Neurosci.*, **17**, 1768–1776.
Volgushev, M., Chauvette, S., Mukovski, M. & Timofeev, I. (2006) Precise long-range synchronization of activity and silence in neocortical neurons during slow-wave oscillations. *J. Neurosci.*, **26**, 5665–5672.
van Vreeswijk, C. & Sompolinsky, H. (1996) Chaos in neuronal networks with balanced excitatory and inhibitory activity. *Science*, **274**, 1724–1726.
Wolfe, J., Houweling, A.R. & Brecht, M. (2010) Sparse and powerful cortical spikes. *Curr. Opin. Neurobiol.*, **20**, 306–312.